Polymer Bulletin
https://doi.org/10.1007/s00289-024-05494-5

ORIGINAL PAPER

Development and characterization of a simple and fast castor oil-based polyurethane coating

Lucas Repecka Alves[1] · Giovanni Miraveti Carriello[1] · Guilherme Manassés Pegoraro[1] · David Rodrigues Gomes[2] · Maira de Lourdes Rezende[2] · Aparecido Junior de Menezes[1]

Received: 26 April 2024 / Revised: 24 August 2024 / Accepted: 4 September 2024

Abstract

This study focuses on the development and characterization of polyurethane coatings using castor oil as a renewable source. Most castor oil-based polyurethane paints have a rather long curing process. Therefore, this study focused on the preparation of a polyurethane paint based on raw castor oil without the need for chemical modifications, in a quick and cost-effective manner. The methodology involved the preparation of the paint using castor oil, isocyanate, calcium carbonate, titanium dioxide, additives and solvents. The coatings were then characterized and compared with industrial polyurethane paint in terms of thermal properties, rheology, UV degradation, adhesion, water resistance, and resistance to salt spray corrosion. Results showed that the castor oil-based paint exhibited comparable rheological behavior to the commercial paint, with superior thermal stability. However, the industrial paint showed better performance in UV degradation and similar behavior in the adhesion tests. In the water resistance test, the castor oil-based paint proved to be superior to the commercial paint. The salt spray corrosion test revealed that the castor oil-based paint had superior corrosion resistance due to the higher proportion of castor oil in the formulation, which increases the crosslinking of the chains. This work offers a simple and fast method to prepare and substitute petrochemical polyols with castor oil in order to use renewable sources with promising properties.

Keywords Polyurethane · Castor oil · Coatings · Polymers

✉ Lucas Repecka Alves
lucasrepecka@estudante.ufscar.br

[1] Materials Laboratory, Graduate Program in Materials Science, Federal University of São Carlos, Sorocaba, SP 18052-780, Brazil

[2] Polymeric Materials Characterization Laboratory, José Crespo Gonzales Faculty of Technology, Sorocaba, SP 18013-280, Brazil

Published online: 19 September 2024

Introduction

Polyurethanes (PUs) are polymers resulting from the reaction between chemical groups containing isocyanate (-NCO) and another chemical substance with groups (-OH). The result of this reaction is the formation of the polymer,whose structure is present in the most diverse materials from this reaction, such as foams, thermoplastics, adhesives, sealants, elastomers and also in paints. Although PUs, in their various forms, have excellent properties and a wide range of applications, these materials generally come from petrochemical sources, and their production ends up accentuating the unwanted effects of global warming due to greenhouse gas emissions. There is also growing global concern about the increasing dependence on resources derived from fossil sources, due to the increase in the price of a barrel of oil [1–4].

To mitigate the unwanted effects of reagents from petrochemical sources, polyols can be replaced with substances from renewable sources, such as castor oil. Compared to other vegetable oils, castor oil is a promising alternative for the production of PUs [5, 6]. Castor oil is made up of triglycerides with several fatty acids, with ricinoleic acid being its main constituent, comprising approximately 90% of its composition [7].

The oil has three hydroxyl groups in its structure, which characterizes it as a natural polyol. These characteristics make it a suitable material to be used as a monomer for crosslinking PUs. Furthermore, this vegetable oil has several positive characteristics, such as low toxicity, biodegradability and affordable cost. Furthermore, it is a non-edible oil, which does not affect the global food supply [4, 8]. In addition to being found in several regions with a tropical climate, Brazil stands out as one of the largest producers and exporters of castor oil in the world [9], this boosts its use as a raw material by the industry for the production of polymers [1, 10–12].

PU paints are composed of resin, solvent, pigments and additives, and can use both natural resins based on vegetable oils and synthetic resins. Its purpose is to adhere and form a film on the applied surface. The resin, together with the solvent, plays a crucial role in defining the properties of paints, such as drying, durability and adhesion. Due to their excellent characteristics, such as resistance to corrosion, abrasion, flexibility, fast curing and chemical resistance, PU paints exert considerable influence on the market. These attributes make them widely used as high-performance coatings in the automobile industry and in household appliances in general [13, 14].

The study of polymerization between crude castor oil and isocyanates for the formation of PU paint films is well established. However, many studies use aliphatic isocyanates, which are significantly more expensive compared to aromatic isocyanates, and the film curing process can take 3 to 15 days [15, 16]. Thus, the present work focuses on the preparation of a crude castor oil-based paint in a simple and rapid manner, with film formation in less than 24 h. For this, the PU paint based on castor oil was characterized and compared with industrial PU paint to evaluate its thermal and rheological properties. Ultraviolet degradation, adhesion,

water resistance, and salt spray corrosion resistance tests were conducted for both paints, aiming to use crude castor oil as a promising substitute in the preparation of new, less expensive, and less harmful to the environment PU paints.

Material and methods

Materials

For the preparation of the resin, raw castor oil purchased from QuimisulSC, Brazil, with hydroxyl and acidity indices of 155 and 1.69 mg KOH/g, respectively, and commercial 2,4-diphenylmethane diisocyanate from Redelease, Brazil, were used. Calcium carbonate ($CaCO_3$) AR from Êxodo Científica, Brazil, was used as filler. Commercial rutile titanium dioxide from Brazil was used as pigment, and toluene AR from Mallinckrodt UltimAR was used as solvent. The additives employed were Tween 20 AR from Neon, Brazil, commercial Renex from Brazil, and Cobalt drier Classic Acrilex from Brazil. Finally, for comparison purposes, the two-component aliphatic PU paint Sumatane 355 from Sherwin-Williams was applied. All reagents were used without prior purification.

Preparation of *castor* oil-based polyurethane paint

The castor oil-based paint was prepared based on the methodology developed by Alves (2024) [17], in which a 3^2 factorial design was applied and obtained 9 samples with different characteristics, and the best sample was chosen to continue the analysis. Based on this, below are the main components of the prepared paint.

To prepare the paint, castor oil and isocyanate were added under mechanical stirring at 300 RPM in a plastic beaker. After that, toluene, as a solvent, was added, along with calcium carbonate ($CaCO_3$) and titanium dioxide (TiO_2) to the binder for the purpose of homogenizing the components. And subsequently, additives were added, such as renex (dispersant), tween 20 (humectant), cobalt drier was added, and the mixture was homogenized for 10 min. The paint was then applied to the desired substrate and left to cure at room temperature for 24 h. Table 1 shows the paint components and quantities used.

The preparation of COPUP can be seen in Fig. 1.

Table 1 Composition of castor oil-based polyurethane paint

Coating components	Proportion
Resin	40% castor oil and 20% isocyanate
Filler	2% of $CaCO_3$
Pigment	4% of TiO_2
Additives	0.05% cobalt drier, 1% renex and 0.95% tween 20
Solvent	32% of toluene

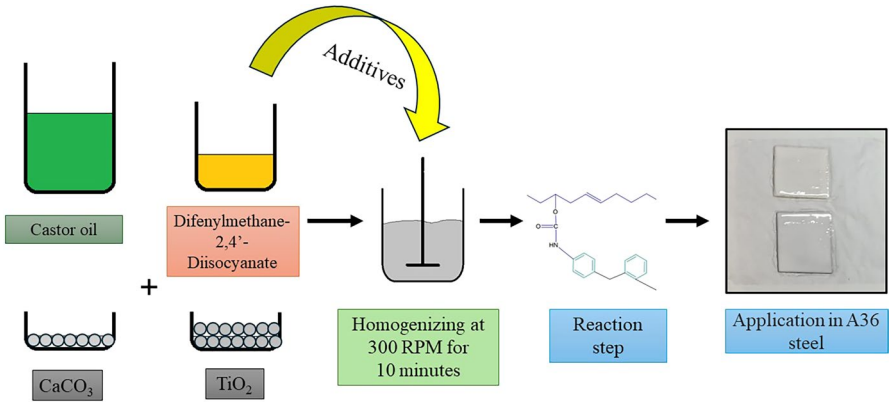

Fig. 1 Graphical representation of the preparation of the castor oil-based paint

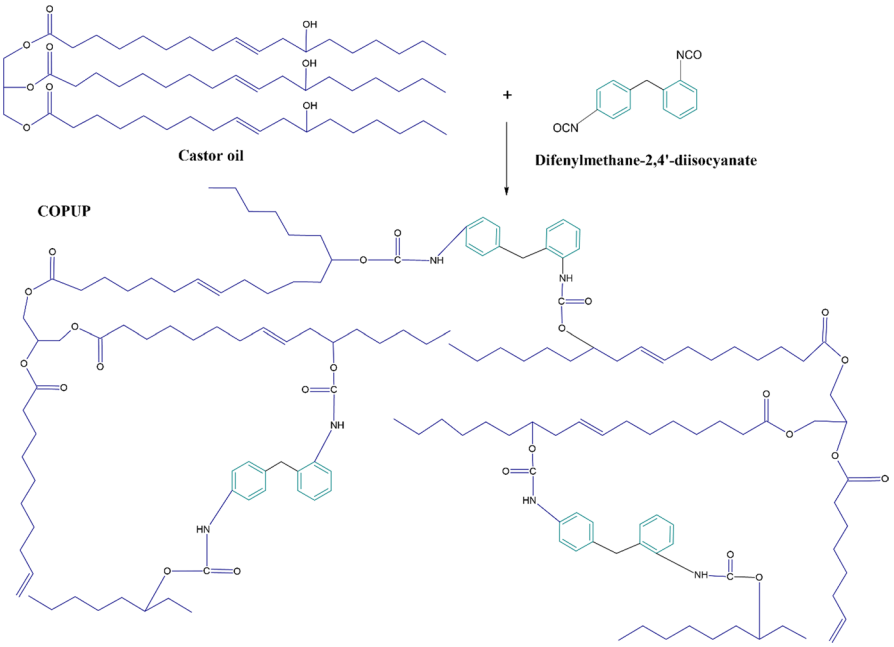

Fig. 2 Representation of the reaction pathway between castor oil and diisocyanate for the formation of the polymeric structure

The synthesis demonstration of COPUP is shown in (Fig. 2).

Preparation of two-component aliphatic PU paint Sumatane 355

The commercial PU paint was prepared according to the manufacturer's instructions, in which 8.6 g of component A and 1 g of component B were weighed into a

plastic container. Subsequently, the paint was stirred at 300 RPM for approximately 5 min to homogenize the components.

Characterization of polyurethane coatings and tests

Fourier-transform infrared spectroscopy (FTIR)

The PU coatings were characterized by FTIR using the PerkinElmer Spectrum 65 spectrophotometer located in the polymer characterization laboratory at the José Crespo Gonzales College of Technology, Sorocaba. To generate the spectra, a resolution of 4 cm^{-1} was used with a 64-scan sweep.

Rheology test

To prove the rheological property of the coating prepared in the laboratory, rheology tests were carried out together with the industrial paint using the DHR-2 rheometer from the TA Instruments brand at the Pontífica Universidade Católica, Sorocaba campus. The tests were carried out at 25 °C using the cone-plate geometry, with a diameter of 40 mm and a spacing of 55 µm. To generate the flow test curves, the apparent viscosity was obtained by varying the shear rate from 10^{-4} to 5.500 s^{-1}. For the thixotropy test, the materials were subjected to three loading blocks varying the shear rate. In the first block, the inks underwent a shear rate of 0.1 s^{-1} for 120 s. Subsequently, the rate was increased to 3.000 s^{-1} where it was applied for 120 s and finally, the rate was reduced to 0.1 s^{-1} being applied for 300 s. And in the frequency sweep test, a controlled shear deformation amplitude of 1% and frequency variation from 0.1 to 500 rad/s were used.

Thermogravimetric analysis (TGA)

To evaluate the thermal properties of coatings, thermogravimetry tests were carried out with the TGA/DTA equipment model 6200 from the brand SII Nanotechnology. The analysis parameters were the following: heating rate: 10 °C/min, temperature range from 25 to 900 °C and nitrogen atmosphere with a flow rate of 100 mL/min.

Differential scanning calorimetry (DSC)

With the purpose of analyzing the thermal transitions of coatings, DSC curves were carried out, the 1st stage being the heating and cooling process with an isotherm of 3 min at 110 °C and subsequent cooling to -90 °C to erase the thermal history. The 2nd stage of heating and cooling were considered for data collection using the DSC 25 equipment from the TA Instruments brand. The analysis parameters were the following: heating rate of 10 °C/min, temperature range from -90 to 110 °C and nitrogen atmosphere with a flow of 50 mL/min. Data were collected using the Trios software.

Optical microscopy

In order to monitor the UV degradation of the paint samples, images were taken every 50 h of exposure using the Leica EZ4W optical microscope coupled to the computer.

Water resistance test

The static immersion test is considered a method for evaluating the water resistance of coatings using the gravimetric method. For this, the samples were immersed in distilled water at a temperature of 25 °C and weighed every 24 h. After that, the samples were dried at 40 °C for one hour in an oven. The mass change was calculated using Eq. 1, where M_1 represents the initial mass of the sample before immersion and M_2 is the final mass after immersion. The data were plotted as a function of time.

$$\Delta M = \frac{M_2 - M_1}{M_1} \times 100\% \tag{1}$$

UV degradation test methodology used in coatings

In order to evaluate the resistance to UV degradation of the prepared coating, two square-shaped substrates with dimensions of 50×50 mm were prepared. The substrates chosen were A36 steel and fiberglass composite with vinyl ester resin. For comparison purposes, two substrates were painted with COPUP and two substrates with IPUP. The wet paint layer thickness was standardized for all samples at 150 µm with the aid of a wet film measuring comb. The UV chamber used for the test was built and adapted according to Vaz et al. (2008) [18]. In order to shorten the test period, UVC lamps with a wavelength of 254 nm were used and every 50 h the samples were taken to an optical microscope in order to evaluate the effects of accelerated aging on the paints, such as the formation of bubbles, cracks, color changes and loss of gloss for 300 h. The test was carried out in triplicate for the two coatings on different substrates.

Paint adhesion test methodology

In order to determine the adhesion of the prepared paints, square-shaped A36 steel substrates measuring 50×50 mm were prepared and painted. The test was carried out using method A, known as X-cut, in accordance with the standard ABNT NBR 11003 [19], which consists of making two cuts of 40 mm in length each, being intercepted in the middle. Subsequently, a 10 cm tape was applied to the center of the intersection. The tape was smoothed with the finger in the areas of the incisions and the tape was rubbed with an eraser in the longitudinal direction, for uniformity

purposes. After 1 to 2 min, the tape was removed at an angle close to 180°. The test was carried out in duplicate for samples without degradation and in sextuplicate for samples degraded at 300 h in UVC in order to verify the adhesion of the samples on the substrate before and after exposure.

Salt spray test methodology for paints

In order to evaluate the corrosion resistance of paint prepared in the laboratory and commercially, the standard NBR 5770 [20], in which a steel substrate measuring 50 × 50 mm was used. The specimens were sanded, washed, dried and painted with a wet paint thickness of 150 µm using the wet film measuring comb. Subsequently, an incision was made in the middle of the sample and the specimens were taken to the equipment. For the test, the Bass equipment LTDA equipment was used with a 5% sodium chloride (NaCl) solution for 1000 h at a controlled temperature of 35 °C. At the end of the test, the pieces were washed and dried. The test was carried out in triplicate for both paints.

Results and discussion

FTIR of *castor* oil based PU paint and industrial paint

Figure 3 displays the FTIR spectrum of castor oil-based paint (COPUP). Initially, the N–H stretching vibration of the intramolecular urethane bond is notable, occurring at about 3337 cm^{-1}. Then, the deformation bands of the CH_3 and CH_2 groups are identified, at 2933 and 2860 cm^{-1}, respectively. The detection of stretching of the carbonyl group at 1730 cm^{-1} indicates the presence of free carbonyl. At around

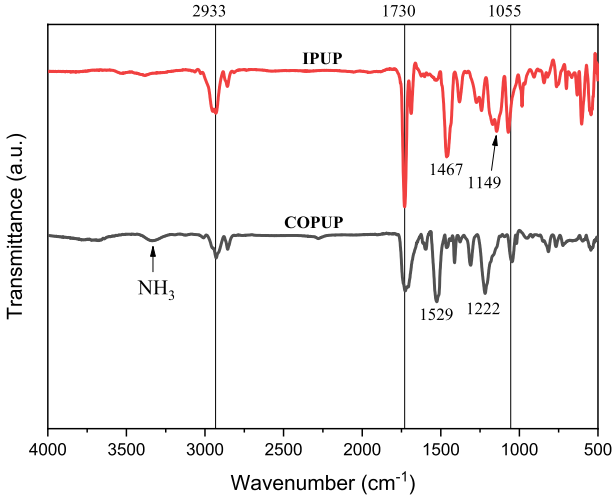

Fig. 3 Infrared spectroscopy of IPUP and COPUP

1529 cm^{-1}, bending vibrations of the N–H bond occur, accompanied by the characteristic band of the C-N bond, at approximately 1312 cm^{-1}. A characteristic band of isocyanurate rings was also observed, around 1414 cm^{-1}. Lastly, the absorption bands at 1220 cm^{-1}, 1100 and 1050 cm^{-1} are attributed to the presence of C–O–C bonds [21–24].

For comparison purposes with the paint prepared in the laboratory, the two-component industrial aliphatic polyurethane paint (IPUP) was characterized. The bands at 2933 and 2864 cm^{-1} are evident, which correspond to the asymmetric and symmetric stretching vibrations of the methylene CH_2 group. Furthermore, it is possible to observe another vibration mode of CH_2 with the appearance of the band at 1467 cm^{-1}. The characteristic frequencies of the urethane bond are observed at 1732 cm^{-1}, where the C = O stretching vibration of the ester overlaps the urethane bond, resulting in a peak with high intensity. The stretching at 1149 cm^{-1} is related to the C–O–C group, while the one at 1055 cm^{-1} is related to the C–N group. The peak at 1246 cm^{-1} is attributed to the amide III band, while the peak at 1522 cm^{-1} refers to the amide II band [20, 21]. It is important to highlight that the appearance of neither the absorption band of the NCO group in the range of 2250 to 2270 cm^{-1} nor of hydroxyl groups in the region of 3500 cm^{-1} was observed. This suggests that the reaction was complete, without the presence of any remaining groups. Thus, it can be stated that the PU paints were successfully synthesized, both for laboratory preparation and for industrial use [25].

Flow rheology test

The flow rheology test aims to analyze the behavior of apparent viscosity over a wide range of shear rates. In the flow test, it is desirable for paints to maintain high viscosity at low shear rates, as this characteristic ensures good sedimentation resistance properties and pigment stability during storage [27].

Analyzing (Fig. 4), it can be seen that IPUP presented greater stability to sedimentation, as its apparent viscosity is greater at low shear rates, which is not observed for COPUP, which demonstrated a lower viscosity under the same conditions. The higher apparent viscosity of IPUP can be explained by the high amount of inorganic fillers in its composition, as demonstrated in Table 2 in the thermogravimetry test, which can result in a higher apparent viscosity. However, the higher apparent viscosity under low shear rates may result in greater difficulty in leveling the applied layers of IPUP, in relation to COPUP. Comparing both paints, COPUP is easier to apply, due to a lower apparent viscosity for higher shear rates [27, 28].

It is observed that, even at shear rates lower than 2 s^{-1}, IPUP presented a higher value of apparent viscosity, indicating a rheological behavior that is more favorable to the resistance to separation of components and paint flow. However, after shear rates greater than 2 s^{-1}, IPUP did not demonstrate a significant reduction in apparent viscosity compared to COPUP, which may make it difficult to apply by brushes, rollers or spray. In the case of COPUP, there is a greater probability of sedimentation occurring at low shear rates [27].

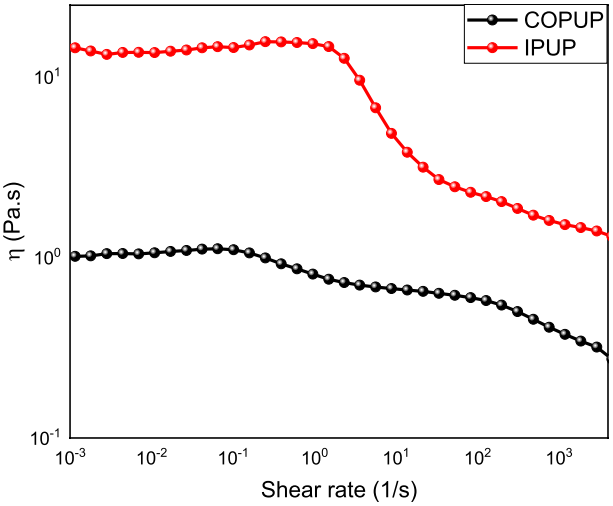

Fig. 4 Flow test

It is important to highlight that both paints exhibited a rheological behavior typical of non-Newtonian fluids, that is, the viscosity decreased as the shear rate increased, indicating pseudoplastic behavior, which is an expected behavior for paints [29].

Thixotropy Test (3ITT)

The three-interval thixotropy test model (3ITT), demonstrates very closely a real scenario of applying paints using brushes or rollers, which represent the loading, lamination and consequent leveling of the paint flow ink [27, 30]

Fig. 5 Thixotropy assay (3ITT)

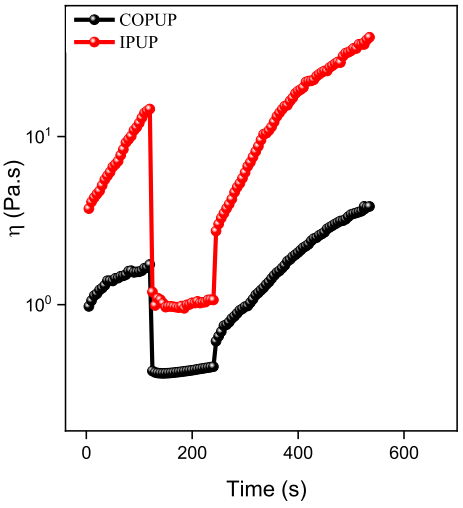

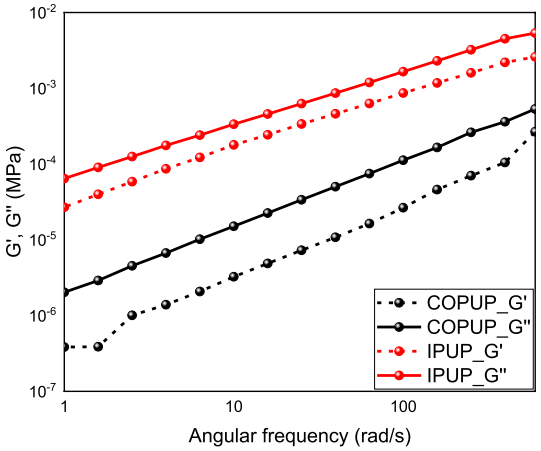

Fig. 6 Frequency sweep test

When examining (Fig. 5), it is noted that IPUP had a higher initial apparent viscosity compared to COPUP. It is also evident that, for both coatings, the shear rate of 3000 s^{-1} resulted in a significant decrease in apparent viscosity, with this reduction being more pronounced for IPUP. Subsequently, when reducing the shear rate, a recovery of the apparent viscosity is observed for both coatings, with this recovery being faster for the IPUP paint [27].

The apparent viscosity under a shear rate of 3000 s^{-1} was close to 1 for IPUP and close to 0.4 for COPUP. Therefore, high shear rates result in lower viscosity values, a desirable property for paints. This indicates greater ease of application using various instruments, such as rollers, brushes and also sprays [27].

Thus, both IPUP and COPUP showed a very pronounced and similar thixotropic behavior, due to the significant variation in apparent viscosity at high shear rates

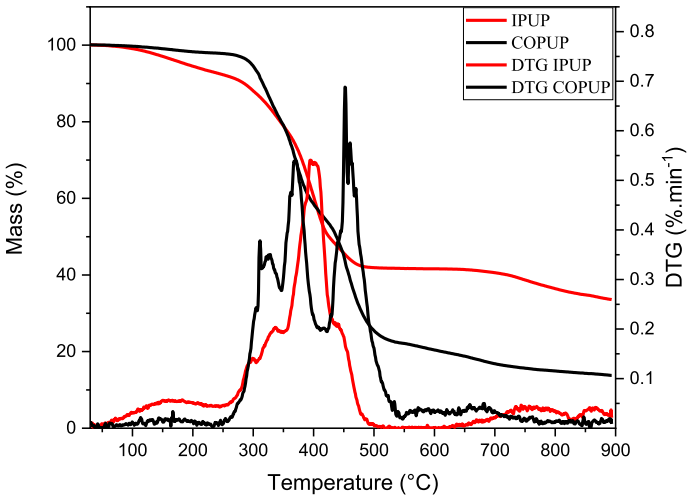

Fig. 7 TG-DTG curves for paints

and the slow and non-linear recovery with the reduction of this rate over time. IPUP demonstrated a recovery of approximately 100% of its viscosity in about 5 s, faster than COPUP. Therefore, COPUP has a greater tendency to flow compared to IPUP, as COPUP has a lower apparent viscosity during the three intervals [27, 30].

Frequency sweep test

As illustrated in (Fig. 6), it is observed that none of the two paints presented storage modulus (G') values higher than the loss modulus (G'') at all frequencies. This behavior differs from that reported by [27], which may suggest a greater resemblance to a liquid than a solid under small deformations. In other words, in this case, viscous behavior prevails over elastic behavior. Therefore, both paints do not maintain a stable shape and can flow easily even at very low viscosities. This can lead to a lower degree of stability, with the possibility of sedimentation and phase separation of these paints during the storage period [31].

It was also noticed that the paints had practically parallel G' and G'' values; however, G' was not higher than G'' at any of the frequencies investigated, which may indicate less stability between the two paints [27].

Thermogravimetry and coating derivative (TG-DTG)

In (Fig. 7), the TG and DTG curves of COPUP and IPUP inks are shown. It is observed that COPUP demonstrated superior thermal resistance to IPUP, as COPUP maintained thermal stability up to 297 °C, with approximately 5% mass loss, while IPUP showed a mass loss of 5% at around 185 °C, in the range between 73.20 to 255.77 °C. Thus, it is noted that IPUP exhibited a considerably anticipated mass loss, which may be an undesirable property for certain applications where higher temperatures are expected. It is also important to highlight that COPUP presented superior thermal stability than the PU paints mentioned in the literature, which exhibit starting decomposition temperatures of around 250 to 284 °C, considering a mass loss of 5% [13, 32, 33].

It can be seen that COPUP presented three well-defined degradation stages, while IPUP presented two. IPUP showed a loss of mass at around 150 °C, which may be related to unreacted products, as well as short chain segments that did not go through the cross-linking process during curing, or even to the evaporation of moisture and volatile molecules present in the sample [34, 35].

The first stage of degradation is associated with the degradation of the rigid segments, due to the low thermal stability of the urethane groups, while the second and third stages are related to the thermal decomposition of the flexible segments, which have more robust chemical bonds [36].

When observing Table 2, it is noted that, during the two stages of thermal degradation for both samples, COPUP exhibited greater thermal stability and lower mass loss for each stage of degradation. However, when analyzing the residual mass of each sample, it appears that IPUP presented a significantly higher amount of inorganic residual mass than COPUP, suggesting that IPUP possibly contains a high

Table 2 Initial and Tmax values for paint samples with decomposition and mass loss temperatures

Samples	1st Step			2nd Step			3rd Step		
	T_{onset} (°C)	T_{max} (°C)	Mass loss (%)	T_{onset} (°C)	T_{max} (°C)	Mass loss (%)	T_{onset} (°C)	T_{max} (°C)	Remaining mass at 900 °C (%)
COPUP	260.97	311.47	8.55	349.19	370.68	29.92	424.98	453.07	13.79
IPUP	73.20	294.31	11.29	346.68	394.90	35.61	–	–	34.90

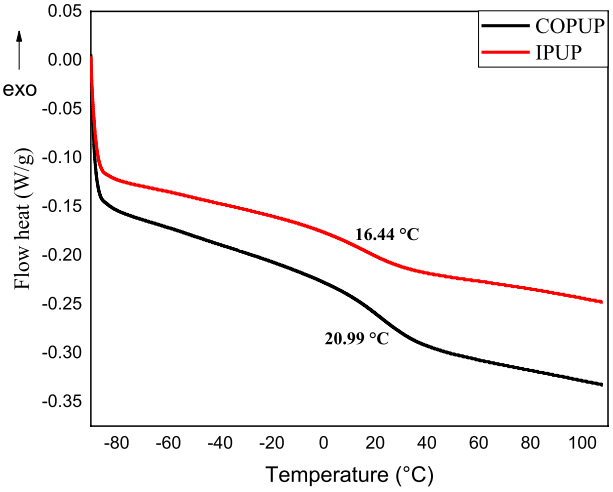

Fig. 8 DSC curves of the paints from the 2nd run

amount of fillers in its composition that act as reinforcements. Some authors [13] indicate that a greater amount of mass residues in paints suggests the presence of several thermostable units that are part of the binder component.

The greater thermal stability of COPUP compared to IPUP can be attributed to the presence of fillers, such as $CaCO_3$, which can function as a thermal insulator, improving the thermal stability of the material. Furthermore, these fillers can provide a barrier effect, delaying the release of volatile compounds originating from the thermal decomposition process [32, 34, 36].

It is also important to highlight the presence of the pigment TiO_2, which, according to studies reported by other researchers, can delay the beginning of the

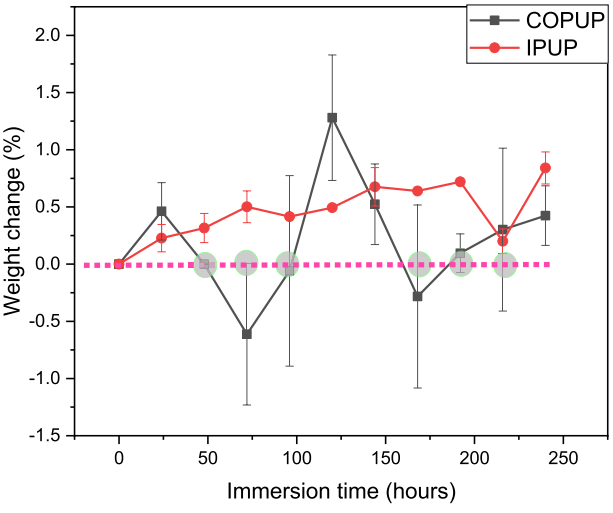

Fig. 9 Mass variations of COPUP and IPUP plotted as a function of immersion time

decomposition process of the material, thus contributing to improving its final thermal stability [37].

Differential scanning calorimetry of paints (DSC)

In (Fig. 8), the DSC curves of PU paints are represented. Initially, both inks presented very close glass transition temperature values (Tg): 16.44 °C for the IPUP ink and 20.99 °C for the COPUP ink. The analyzes indicated that the paints have an amorphous structure, as no thermal events were observed, such as crystallization and melting peaks. Knowing the Tg value of polymers, especially in paints, is extremely important, as these materials do not show mobility at temperatures below their respective Tgs. Therefore, it can be inferred that COPUP ink has greater dimensional stability compared to IPUP [38].

According to the observations of Kathalewar et al. (2013) [39], different types of isocyanates can result in different Tg values for PUs, especially HDI, used in IPUP paint, which can lead to less crosslinking of the material and, consequently, a lower Tg compared to COPUP, in which it was MDI was used as a hardener. Furthermore, it is important to highlight that PU paints prepared with HDI generally have a Tg of around 10 to 20 °C, which is in agreement with experimentally obtained data [40].

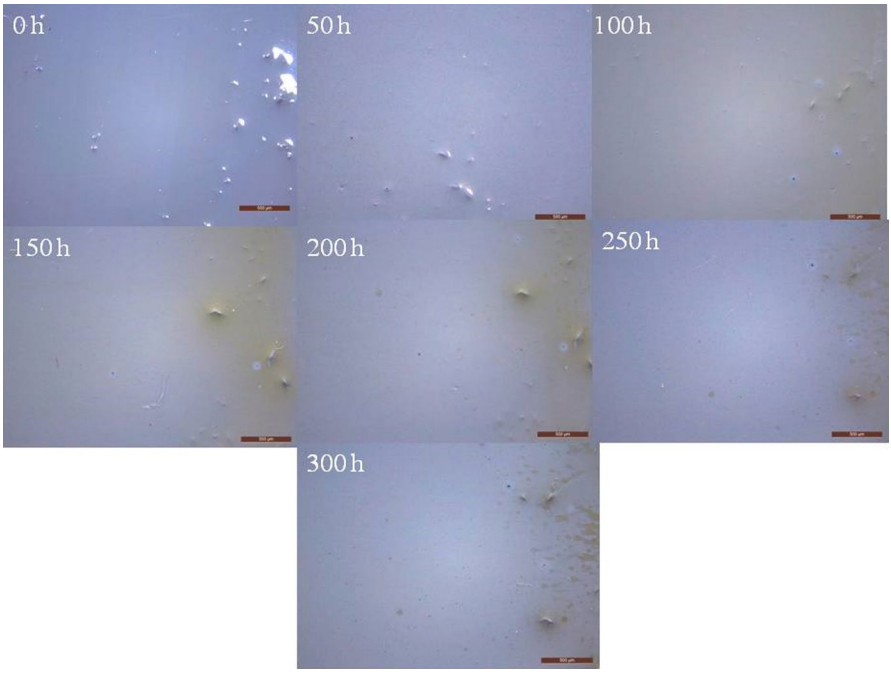

Fig. 10 Images of industrial paint applied to A36 steel substrate exposed to 0, 50, 100, 150, 200, 250 and 300 h under UVC

Water resistance of coatings

Figure 9 presents the mass change curves over time for COPUP and IPUP. PUs generally have a strong tendency to absorb water, which can compromise the performance of the coating and lead to a loss of adhesion to the substrate. The paints used in this study are composed of resin, additives, and fillers, components that may affect the water resistance of each formulation [41, 42].

When analyzing COPUP, a significantly different behavior is observed compared to IPUP, where both apparent mass gains and losses are noted. Considering the error, it is evident that the uncertainty is greater than the measured magnitude for COPUP during the time intervals of 72, 96, 168, 192, and 216 h. Therefore, it is not possible to statistically assert that there was a significant variation in mass for the samples during these intervals. However, considering the mass variation for the intervals where the uncertainty was not greater than the magnitude, COPUP absorbed approximately 2.7% of water during the 240 h of testing. Consequently, COPUP exhibited excellent water resistance, which can be attributed to a less permeable surface of the sample, as well as the hydrophobicity of the castor oil chains [43].

In comparison, IPUP exhibits behavior quite different from that observed in COPUP, where mass gains, despite some variations, showed a certain linearity.

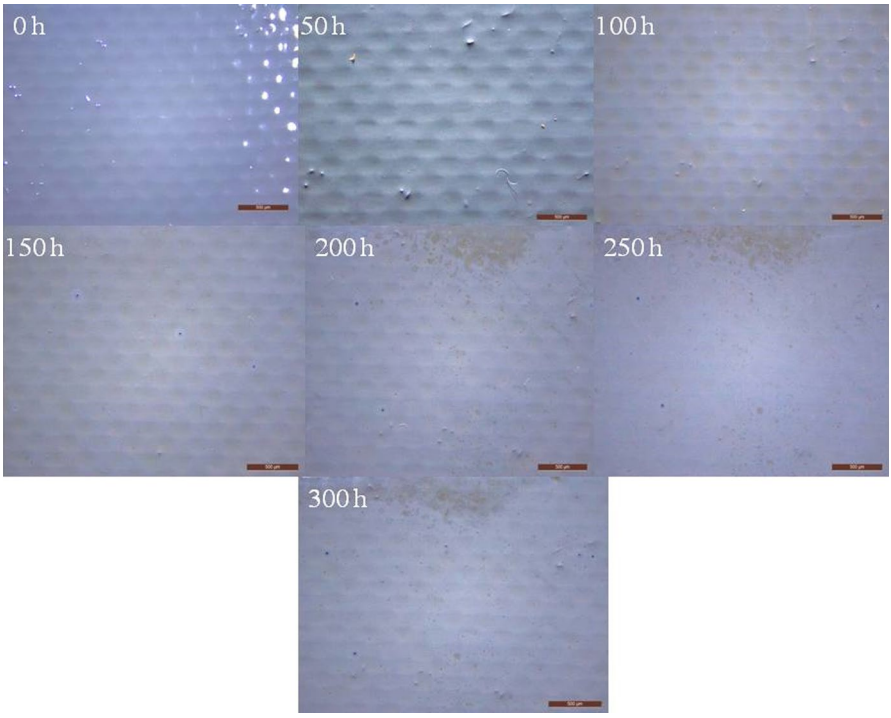

Fig. 11 Images of the industrial paint applied to the fiberglass composite substrate with vinyl ester resin exposed to 0, 50, 100, 150, 200, 250 and 300 h under UVC

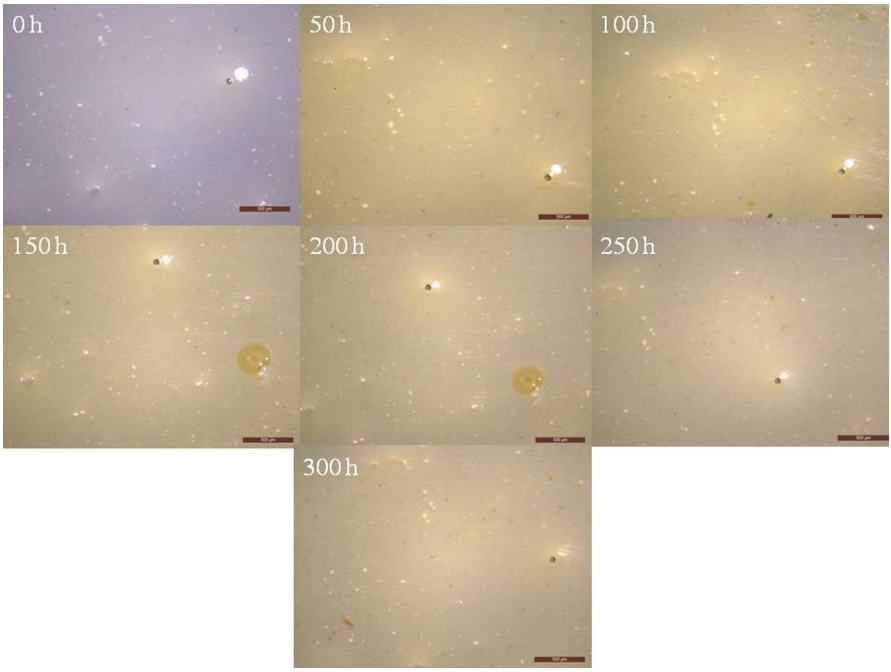

Fig. 12 Images of castor oil-based paint applied to A36 steel substrate exposed to 0, 50, 100, 150, 200, 250 and 300 h under UVC

Considering the measured error, it is evident that IPUP did not exhibit, at any time interval, an uncertainty greater than its magnitude, indicating that the material indeed absorbed more water compared to COPUP, absorbing approximately 5% of water during the 240 h of testing. This observed behavior may be related to its composition, such as a less dense network structure, which allows for greater water penetration. Thus, COPUP exhibited superior water resistance compared to IPUP [41].

Optical microscopy of industrial polyurethane paint

The optical microscopy images illustrated the main aspects of degradation of industrial PU paint and that prepared in the laboratory, applied to A36 steel substrates and vinyl ester resin with fiberglass, as shown in (Fig. 10).

In the first 50 h of UVC degradation, it is noted that the industrial paint applied to A36 steel practically showed no significant change in color. However, upon reaching 100 h of testing, the paint exhibited a marked loss of brightness, along with the appearance of brown spots and small bubbles. When the test reached 150 h, these characteristics became even more evident, and the paint practically lost all its shine, presenting a very matte finish. Finally, between 200 and 300 h, a greater prevalence of small bubbles on the paint surface was observed. The results observed for the industrial paint are in accordance with data reported in the literature, as aliphatic

PUs do not exhibit significant discoloration, since they do not have a sequence of several π bonds that could act as chromophores, thus altering the color of the material [44].

The industrial paint applied to the vinyl ester resin substrate with fiberglass in (Fig. 11) showed similar behavior to the paint applied to steel. In the first 50 h of testing, the paint lost its brightness, and during the 100 h of degradation, small brown spots appeared. Upon reaching 150 h, small bubbles appeared, and at 200 h, dark brown spots appeared, similar to the phenomenon that occurred with paint applied to steel. Between 250 and 300 h, these characteristics intensified. These phenomena, such as the formation of bubbles, loss of gloss and stains, are clear indicators of paint degradation caused by accelerated aging. The small color variation of the ink when exposed to UV radiation can be associated with the good resistance to UV degradation provided by HDI to the paint [45].

Optical microscopy of *castor* oil-based polyurethane paint

For the castor oil-based PU paint applied to A36 steel in (Fig. 12), it can be seen that in the first 50 h of testing, the paint already showed a change in color, acquiring a yellowish tone.

The yellowing can be explained by the presence of aromatic rings in the PU structure. When these rings absorb electrons, the polymer is isomerized to an

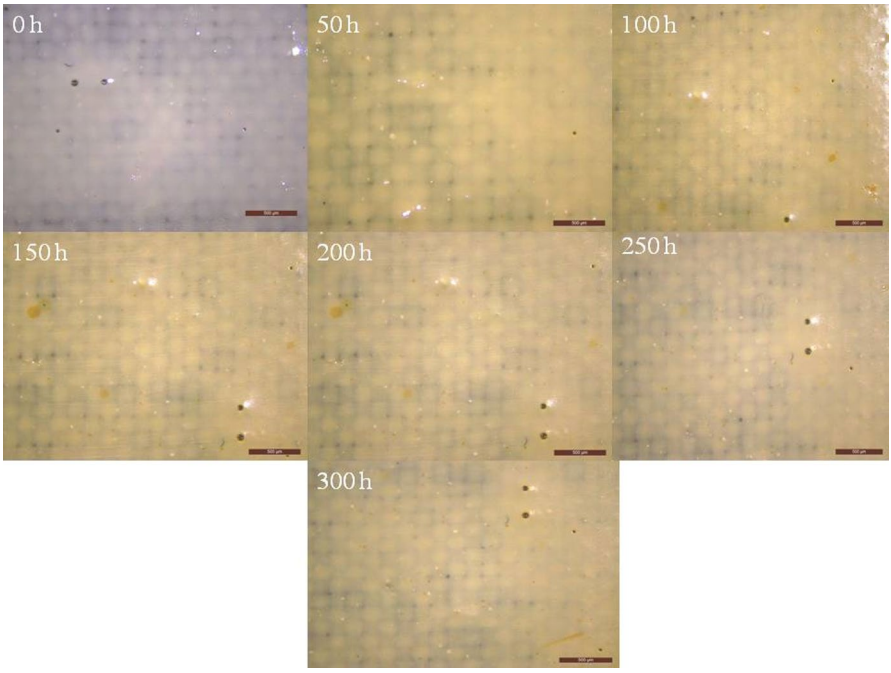

Fig. 13 Images of castor oil-based paint applied to fiberglass composite substrate with vinyl ester resin exposed to 0, 50, 100, 150, 200, 250 and 300 h under UVC

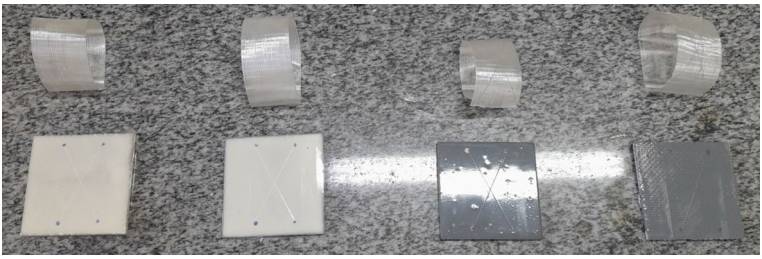

Fig. 14 Adhesion test for non-degraded samples of COPUP on the left and IPUP on the right

enol form, as it has three interspersed double bonds, which results in yellowing. Furthermore, this phenomenon is also associated with the scission of urethane groups and the photooxidation of groups, such as CH_2, which are located between the aromatic rings of the polymer structure. Oxidation of the urethane bond produces the quinone-imide structure, which acts as a chromophore responsible for the yellowing of the material [44, 46, 47].

Upon reaching 100 h of testing, it is possible to notice small circle-shaped yellow spots. This phenomenon can be explained by the formation of radicals arising from the oxidation of the flexible PU segments, especially the polyester present in castor oil, which can also contribute to the oxidation of aromatic urethane bonds by subtracting the hydrogen present in the carbon atom. from the CH_2 group. Upon reaching 150 and 200 h of exposure, these characteristics become

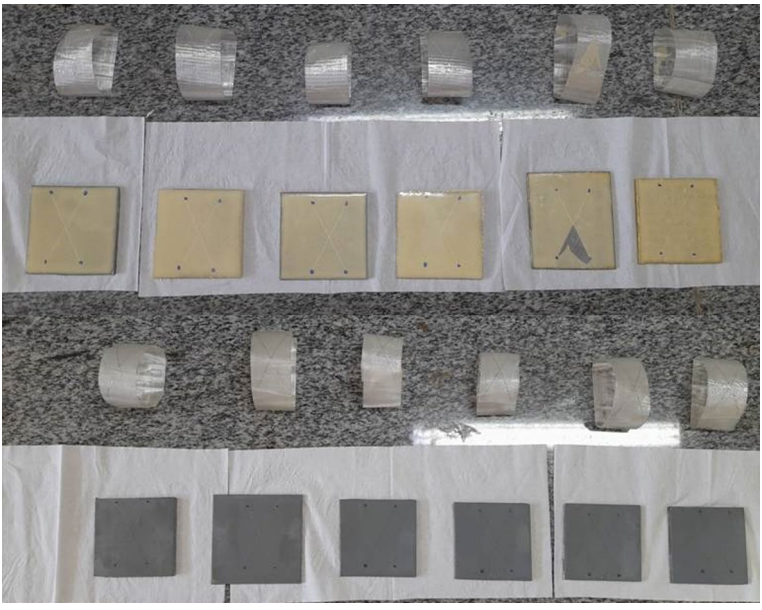

Fig. 15 Adhesion test for degraded COPUP and IPUP samples

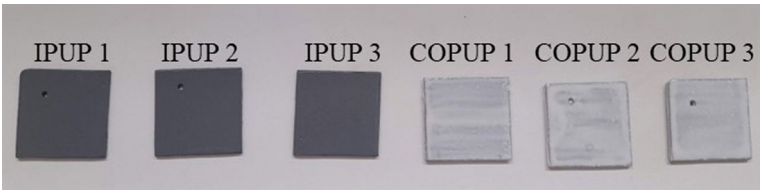

Fig. 16 Industrial paint on the left and castor oil-based paint on the right before salt spray testing

Table 3 Degree of corrosion for castor oil-based paint and industrial paint

Coating	Degree of rusting (ASTM 610)	Degree of rusting (ABNT NBR 15239)
COPUP 1	6-S	Degree 6
COPUP 2	2-S	Degree 4
COPUP 3	3-S	Degree 6
IPUP 1	1-G	Degree 0
IPUP 2	1-G	Degree 0
IPUP 3	1-G	Degree 0

more expressive, accompanied by a greater loss of brightness and a new change in color, changing to a lighter yellowish tone. Between 250 and 300 h, the yellow spots are no longer evident. Although the paint showed a loss of gloss throughout exposure to UV radiation, the castor oil-based paint showed less loss of gloss when compared to the industrial paint throughout the accelerated aging period [47].

The castor oil-based PU paint applied to the vinyl ester resin substrate with glass fiber showed degradation characteristics similar to those observed when applied to steel, as can be seen in (Fig. 13).

Among these characteristics, yellowing can also be highlighted, due to photoxidation and scission of urethane groups, which was also observed in the first 50 h of degradation on the steel substrate [46, 48].

After 100 h, yellow spots appear on the substrate resulting from the oxidation of the flexible segments of castor oil. Between 150 and 300 h, the color change to a lighter tone is evident, the same event that occurred with the paint applied to the steel. It is important to highlight that, although COPUP showed an evident color change within a few hours of exposure, the paint managed to maintain a shiny appearance, unlike industrial paint, however, it showed the formation of larger bubbles than those presented by industrial paint. Therefore, paint containing MDI as isocyanate presents a limitation regarding its use in external applications where color is a preponderant factor, as it is quite sensitive to photodegradation [47, 48].

Determination of adhesion of non-degraded samples

From (Fig. 14) for the non-degraded samples, it is possible to observe that they did not show detachment at the intersection, nor along the incisions. This corresponds to codes Y0 and X0, according to the ABNT NBR 11003 standard, demonstrating that both COPUP and IPUP presented excellent adhesion on the substrates. This result can be attributed to the fact that COPUP was prepared with a higher ratio of castor oil responsible for the flexible segment in relation to isocyanate, which is in accordance with [49]. The authors claimed that greater PUP flexibility favors greater mechanical adhesion to the substrate, as discussed by [50].

Determination of adhesion of samples degraded in UVC

According to (Fig. 15), in the adhesion test for samples degraded in 300 h under UVC, it can be seen that only one COPUP sample showed peeling just below the intersection, corresponding to codes Y_4 and X_1.

This may have been caused by the lack of uniformity during tape removal, since the other five samples did not show any detachment at the intersection, only showing detachment of up to 1 mm along the incisions, which corresponds to code Y_0 and X_1. It is worth highlighting that, despite the phenomenon discussed about yellowing on the surface of COPUP being related to the degradation of the material, the vegetable-based paint did not show significant losses of adhesion on the substrate, and this result is corroborated with the results obtained by [51]. The authors evaluated the exposure of PUs under UV and noticed that after a long period of exposure, the PU underwent greater cross-linking in its chains, which can improve the mechanical resistance properties of the material, as discussed.

In comparison, the IPUP samples showed no detachment at the intersection and also only detachment of up to 1 mm along the incisions, being code Y_0 and X_1 for these samples. Therefore, it can be stated that even after exposure to ultraviolet, the

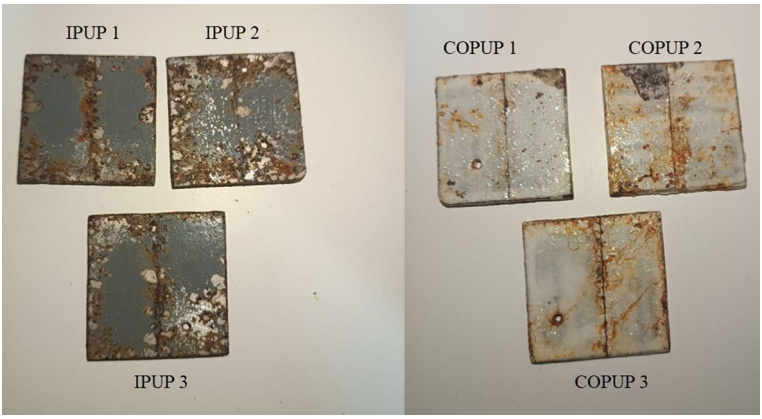

Fig. 17 Industrial paint on the left and castor oil-based paint on the right after 1000 h of exposure to the salt spray chamber

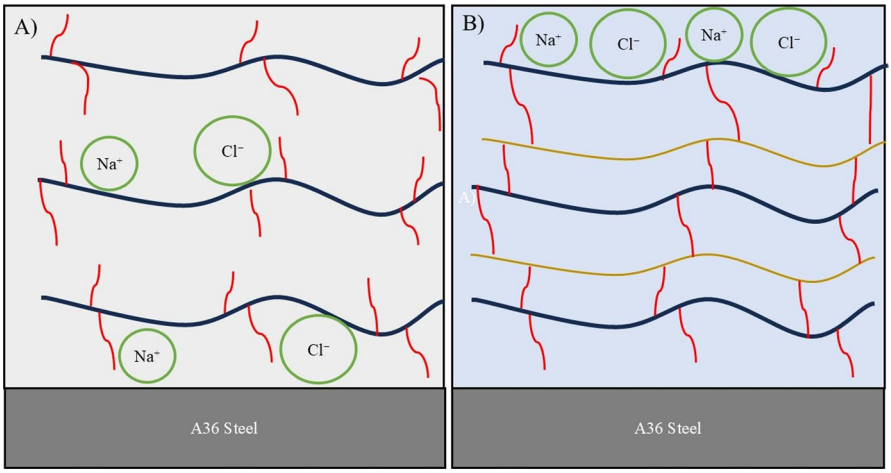

Fig. 18 Possible mechanism for corrosion protection by the film. (**a**) IPUP film and (**b**) COPUP film with a high degree of crosslinking

samples exhibited excellent adhesion, both for COPUP and IPUP. In view of this, it can be stated that the vegetable-based paint demonstrated adhesion properties very similar to industrial PU paint, which are known for their good adhesion to the substrate, as discussed [52].

Salt spray test

In (Fig. 16), it is showed the industrial PU paint on the left and the castor oil-based PU paint on the right before the test.

Table 3 presents the performance results of the degree of corrosion of the substrates, in accordance with ASTM D610 and ABNT NBR 15239, and qualitatively between them. It is notable to note that the industrial PU paint showed the highest degree of corrosion on the substrate of the painted sample compared to the castor oil-based PU paint, as the denomination of the 1-G and Degree 0 results of the industrial paint is resulting from intense corrosion and the existence of delamination of the paint from the substrate, on the other hand, for the castor oil-based PU paint, the results were 6-S and Degree 6, where it had a low percentage of corrosion, there is no evidence of paint delamination [51, 53–55].

In (Fig. 17) it is possible to notice the degree of corrosion of the test specimens coated with aliphatic polyurethane paints on the left and castor oil-based polyurethane paints on the right. There is a noticeable difference in behavior between the formulations, especially in relation to the adhesion of the paint to the substrate. When comparing the castor oil-based polyurethane paint with the aliphatic polyurethane paint, it is noted that in the latter there was delamination of the film in relation to the substrate, while the castor-based paint showed better corrosion resistance [13].

The degradation that occurred in the aliphatic polyurethane paint results from the absence of the aromatic ring, which facilitates the penetration of the NaCl electrolyte, causing the hydrolysis of the coating, that is, the scission of the chains [13]. Dissolving the pigment with NaCl causes the coating to perforate, intensifying the migration of corrosive species onto the A36 steel interface, which consequently generates degradation in the form of micropores [53]. This phenomenon, therefore, can create channels that accelerate the arrival of aggressive ions on the metal substrate, resulting in intense corrosion [53].

The superior corrosion resistance of castor oil-based paint compared to commercial paint can be explained by the higher proportion of castor oil to isocyanate in the paint preparation and the superior water resistance compared to IPUP, which hinders water penetration into the substrate. This can generate remaining hydroxyl groups, which end up increasing the crosslinking degree of the material's chains, making the paint film more compact and offering greater resistance to corrosion by certain ions, such as Na^+ and Cl^-, which have more difficulty penetrating the crosslinked polymer network to the metallic substrate, thus improving the salt spray resistance of the coating. This demonstrative mechanism can be observed in (Fig. 18) [56, 57].

Conclusion

In the present work, it was possible to note that castor oil successfully replaced the petrochemical source polyol for the preparation of the paint, through the main PU reference bands through the FTIR spectrum. Rheology tests revealed that the industrial paint had superior performance, while the castor oil-based paint exhibited rheological behavior comparable to the commercial paint, thus confirming the success in preparing the vegetable-based paint. In the TG test, vegetable-based paint was thermally superior to industrial paint. For the DSC test, COPUP demonstrated greater dimensional stability than IPUP. In the UV degradation analysis, the commercial paint proved to be superior to the castor oil-based paint, as it did not exhibit a significant color change. However, in the adhesion test, the vegetable-based paint showed very satisfactory performance, comparable to that of the industrial paint. In the water resistance test, COPUP outperformed IPUP, as the coatings absorbed 2.7 and 5% of water, respectively. Finally, in the salt spray test, COPUP showed superior corrosion resistance to IPUP, which makes vegetable-based paint an economically viable and less harmful option for replacing industrial PU paint.

Acknowledgements This study was financed in part by the Coordenação de Aperfeiçoamento de Pessoal de Nível Superior—Brasil (CAPES)—Finance Code 001.

Author's contribution All authors contributed to the study conception and design. Material preparation, data collection and analysis were performed by LRA, GMC, GMP, DRG, MLR and AJM. The first draft of the manuscript was written by LRA, GMC, GMP and DRG and all authors commented on previous versions of the manuscript. All authors read and approved the final manuscript.

Data availability No datasets were generated or analysed during the current study.

Declarations

Conflict of interest The authors declare that there is no conflict of interest regarding the publication of this article

References

1. Paraskar PM, Prabhudesai MS, Hatkar VM, Kulkarni RD (2021) Vegetable oil based polyurethane coatings—a sustainable approach: a review. Prog Org Coat 156:106267. https://doi.org/10.1016/j.porgcoat.2021.106267
2. Alves LR, Carriello GM, Pegoraro GM, Lopes HSM, de Janolla TA, Dias ANC, Mambrini GP, de Rezende ML, de Menezes AJ (2023) Synthesis and characterization of polyurethane and samarium(III) oxide and holmium(III) oxide composites. Polímeros 33:e20230039. https://doi.org/10.1590/0104-1428.20230023
3. Patil CK, Rajput SD, Marathe RJ, Kulkarni RD, Phadnis H, Sohn D, Mahulikar PP, Gite VV (2017) Synthesis of bio-based polyurethane coatings from vegetable oil and dicarboxylic acids. Prog Org Coat 106:87–95. https://doi.org/10.1016/j.porgcoat.2016.11.024
4. Repecka Alves L, Miraveti Carriello G, Manassés Pegoraro G, Moraes CE, de Lourdes Rezende M, de Menezes AJ (2024) Green polyurethane foams: replacing petrochemical polyol with castor oil through factorial design. J Polym Res 31:227. https://doi.org/10.1007/s10965-024-04077-2
5. Mistry M, Prajapati V, Dholakiya BZ (2024) Redefining construction: an in-depth review of sustainable polyurethane applications. J Polym Environ. https://doi.org/10.1007/s10924-023-03161-w
6. Jariwala S, Desai YN, Sahu P, Gupta RK (2024) Hemp seed oil derived rigid polyurethane foams and their underlying flame retardancy properties. J Polym Environ. https://doi.org/10.1007/s10924-024-03215-7
7. Kaikade DS, Sabnis AS (2023) Recent advances in polyurethane coatings and adhesives derived from vegetable oil-based polyols. J Polym Environ 31:4583–4605. https://doi.org/10.1007/s10924-023-02920-z
8. Patil CK, Jung DW, Jirimali HD, Baik JH, Gite VV, Hong SC (2021) Nonedible vegetable oil-based polyols in anticorrosive and antimicrobial polyurethane coatings. Polymers 13:3149. https://doi.org/10.3390/polym13183149
9. da Silva César A, Otávio Batalha M (2010) Biodiesel production from castor oil in Brazil: a difficult reality. Energy Policy 38:4031–4039. https://doi.org/10.1016/j.enpol.2010.03.027
10. Alves LR, Carriello GM, Pegoraro GM, Filho JF (2021) A utilização de óleos vegetais como fonte de polióis para a síntese de poliuretano: uma revisão. Disciplinarum Scientia | Naturais e Tecnológicas 22:99–118. https://doi.org/10.37779/nt.v22i1.3711
11. Mosiewicki MA, Dell'Arciprete GA, Aranguren MI, Marcovich NE (2009) Polyurethane foams obtained from castor oil-based polyol and filled with wood flour. J Compos Mater 43:3057–3072. https://doi.org/10.1177/0021998309345342
12. Wang HJ, Rong MZ, Zhang MQ, Hu J, Chen HW, Czigány T (2008) Biodegradable foam plastics based on castor oil. Biomacromol 9:615–623. https://doi.org/10.1021/bm7009152
13. Dutta S, Karak N, Jana T (2009) Evaluation of Mesua ferrea L. seed oil modified polyurethane paints. Prog Organic Coat 65:131–135. https://doi.org/10.1016/j.porgcoat.2008.10.008
14. Howarth G (2003) Polyurethanes, polyurethane dispersions and polyureas: past, present and future, surface coatings international part B: coatings. Transactions 86:111–118. https://doi.org/10.1007/BF02699621
15. Macalino AD, Salen VA, Reyes LQ (2017) Castor oil based polyurethanes: synthesis and characterization. IOP Conf Ser Mater Sci Eng 229. https://doi.org/10.1088/1757-899X/229/1/012016
16. Mohanty S, Borah K, Kashyap SS, Sarmah S, Bera MK, Basak P, Narayan R (2023) Development of hydrophobic polyurethane film from structurally modified castor oil and its anticorrosive performance. Polym Adv Technol 34:351–362. https://doi.org/10.1002/pat.5892
17. Alves LR (2024) Preparação, caracterização e aplicação de tinta bicomponente de poliuretano à base de óleo de mamona, Master's thesis, Federal University of São Carlos. https://repositorio.ufscar.br/handle/ufscar/19250 (Accessed 13 Feb 2024)

18. Vaz FAS, de Oliveira MAL, de Queiroz MPG, Ribeiro SJL (2008) Construção de câmara de luz ultravioleta para fotopolimerização de fases estacionárias monolíticas. Quím Nova 31:2156–2158. https://doi.org/10.1590/S0100-40422008000800041
19. T.E. e C. Ltda, ABNT NBR 11003 NBR11003 Pintura industrial—Determinação da, (n.d.). https://www.target.com.br/produtos/normas-tecnicas/34376/nbr11003-pintura-industrial-determinacao-da-aderencia-pelos-metodos-de-corte-na-pintura (accessed March 2, 2024).
20. T.E. e C. Ltda, Target Normas: ABNT NBR 5770 NBR5770 Determinação do grau, (n.d.). https://www.normas.com.br/visualizar/abnt-nbr-nm/2423/nbr5770-determinacao-do-grau-de-enferrujamento-de-superficies-pintadas (accessed March 2, 2024).
21. Jaganathan SK, Mani MP, Ayyar M, Supriyanto E (2017) Engineered electrospun polyurethane and castor oil nanocomposite scaffolds for cardiovascular applications. J Mater Sci 52:10673–10685. https://doi.org/10.1007/s10853-017-1286-0
22. Wang C, Zheng Y, Xie Y, Qiao K, Sun Y, Yue L (2015) Synthesis of bio-castor oil polyurethane flexible foams and the influence of biotic component on their performance. J Polym Res 22:145. https://doi.org/10.1007/s10965-015-0782-7
23. Gurunathan T, Mohanty S, Nayak SK (2015) Isocyanate terminated castor oil-based polyurethane prepolymer: synthesis and characterization. Prog Org Coat 80:39–48. https://doi.org/10.1016/j.porgcoat.2014.11.017
24. Ristić IS, Budinski-Simendić J, Krakovsky I, Valentova H, Radičević R, Cakić S, Nikolić N (2012) The properties of polyurethane hybrid materials based on castor oil. Mater Chem Phys 132:74–81. https://doi.org/10.1016/j.matchemphys.2011.10.053
25. Liu H, Zhang L, Zuo Y, Wang L, Huang D, Shen J, Shi P, Li Y (2009) Preparation and characterization of aliphatic polyurethane and hydroxyapatite composite scaffold. J Appl Polym Sci 112:2968–2975. https://doi.org/10.1002/app.29862
26. Carvalho JED, Claro, S, Neto GO (2014) Chierice, Caracterização térmica do poliuretano derivado de óleo vegetal utilizado para confecção de dispositivo de assistência ventricular. Braz J Therm Anal 3:16. https://doi.org/10.18362/bjta.v3i1-2.21.
27. Machado AML, Noberto CC, Damasceno Filho FE, da Silva WMM, L.F. de A.L. Babadopulos, M.S. Medeiros Júnior, (2021) Estudo comparativo entre os parâmetros reológicos de tintas acrílicas arquitetônicas. Ambient. constr. 22:223–240. https://doi.org/10.1590/s1678-86212022000100589
28. Osterhold M (2000) Rheological methods for characterising modern paint systems. Prog Org Coat 40:131–137. https://doi.org/10.1016/S0300-9440(00)00124-7
29. da Sirqueira AS, Teodoro Júnior D, da Coutinho MS, da Silva Neto AS, dos Silva AA, Soares BG (2016) Rheological behavior of acrylic paint blends based on polyaniline. Polímeros 26:215–220. https://doi.org/10.1590/0104-1428.2178.
30. Bhavsar R, Shreepathi S (2016) Evolving empirical rheological limits to predict flow-levelling and sag resistance of waterborne architectural paints. Prog Org Coat 101:15–23. https://doi.org/10.1016/j.porgcoat.2016.07.016
31. Moolman PL (2008) Rheological model for paint properties, Stellenbosch : Stellenbosch University. http://hdl.handle.net/10019.1/1110 (Accessed 24 Feb 2024).
32. Li B, Li S-M, Liu J-H, Yu M (2014) The heat resistance of a polyurethane coating filled with modified nano-CaCO3. Appl Surf Sci 315:241–246. https://doi.org/10.1016/j.apsusc.2014.07.022
33. Thomas J, Singh V, Jain R (2020) Synthesis and characterization of solvent free acrylic copolymer for polyurethane coatings. Prog Org Coat 145:105677. https://doi.org/10.1016/j.porgcoat.2020.105677
34. Tikhani F, Shirkavand Hadavand B, Fakharizadeh Bafghi H, Jouyandeh M, Vahabi H, Formela K, Hosseini H, Paran SMR, Esmaeili A, Mohaddespour A, Saeb MR (2020) Polyurethane/silane-functionalized ZrO_2 nanocomposite powder coatings: thermal degradation kinetics. Coatings 10:413. https://doi.org/10.3390/coatings10040413
35. Young CN, Clayton CR, Wynne JH, Yesinowski JP, Daniels GC (2015) Physicochemical investigation of chemical paint removers. II: role and mechanism of phenol in the removal of polyurethane coatings. Prog Organic Coat 88:212–219. https://doi.org/10.1016/j.porgcoat.2015.06.014
36. Cervantes-Uc JM, Espinosa JIM, Cauich-Rodríguez JV, Ávila-Ortega A, Vázquez-Torres H, Marcos-Fernández A, San Román J (2009) TGA/FTIR studies of segmented aliphatic polyurethanes and their nanocomposites prepared with commercial montmorillonites. Polym Degrad Stab 94:1666–1677. https://doi.org/10.1016/j.polymdegradstab.2009.06.022

37. Mariappan T, Agarwal A, Ray S (2017) Influence of titanium dioxide on the thermal insulation of waterborne intumescent fire protective paints to structural steel. Prog Org Coat 111:67–74. https://doi.org/10.1016/j.porgcoat.2017.04.036
38. de Camargo M (2002) Resinas poliésteres carboxifuncionais para tinta em pó : caracterização e estudo cinético da reação de cura, Doctoral dissertation. Federal University of Rio Grande do Sul. https://lume.ufrgs.br/handle/10183/2995 (Accessed 25 Feb 2024)
39. Kathalewar M, Dhopatkar N, Pacharane B, Sabnis A, Raut P, Bhave V (2013) Chemical recycling of PET using neopentyl glycol: reaction kinetics and preparation of polyurethane coatings. Prog Org Coat 76:147–156. https://doi.org/10.1016/j.porgcoat.2012.08.023
40. Pan X, Webster DC (2012) New biobased high functionality polyols and their use in polyurethane coatings. Chemsuschem 5:419–429. https://doi.org/10.1002/cssc.201100415
41. Wang Z, Han E, Ke W (2006) An investigation into fire protection and water resistance of intumescent nano-coatings. Surf Coat Technol 201:1528–1535. https://doi.org/10.1016/j.surfcoat.2006.02.021
42. Qiao X, Chen R, Zhang H, Liu J, Liu Q, Yu J, Liu P, Wang J (2019) Outstanding cavitation erosion resistance of hydrophobic polydimethylsiloxane-based polyurethane coatings. J Appl Polym Sci 136:47668. https://doi.org/10.1002/app.47668
43. Liang H, Wang S, He H, Wang M, Liu L, Lu J, Zhang Y, Zhang C (2018) Aqueous anionic polyurethane dispersions from castor oil. Ind Crops Prod 122:182–189. https://doi.org/10.1016/j.indcrop.2018.05.079
44. Bruno GU (2018) Avaliação da degradação natural e acelerada de revestimentos orgânicos. Master's thesis, Federal University of Rio Grande do Sul. https://lume.ufrgs.br/handle/10183/179540 (Accessed 25 Feb 2024)
45. Gomez CM, Gutierrez D, Asensio M, Costa V, Nohales A (2017) Transparent thermoplastic polyurethanes based on aliphatic diisocyanates and polycarbonate diol. J Elastomers Plast 49:77–95. https://doi.org/10.1177/0095244316639633
46. Scholz P, Wachtendorf V, Panne U, Weidner SM (2019) Degradation of MDI-based polyether and polyester-polyurethanes in various environments—effects on molecular mass and crosslinking. Polym Testing 77:105881. https://doi.org/10.1016/j.polymertesting.2019.04.028
47. Xie F, Zhang T, Bryant P, Kurusingal V, Colwell JM, Laycock B (2019) Degradation and stabilization of polyurethane elastomers. Prog Polym Sci 90:211–268. https://doi.org/10.1016/j.progpolymsci.2018.12.003
48. Zia KM, Bhatti IA, Barikani M, Zuber M (2008) Islam-ud-Din, Surface characteristics of UV-irradiated polyurethane elastomers extended with α, ω-alkane diols. Appl Surf Sci 254:6754–6761. https://doi.org/10.1016/j.apsusc.2008.04.066
49. Hormaiztegui MEV, Daga B, Aranguren MI, Mucci V (2020) Bio-based waterborne polyurethanes reinforced with cellulose nanocrystals as coating films. Prog Org Coat 144:105649. https://doi.org/10.1016/j.porgcoat.2020.105649
50. (2015) Tuning the mechanical performance and adhesion of polyurethane UV cured coatings by composition of acrylic reactive diluents. Prog Organic Coat 89: 288–296. https://doi.org/10.1016/j.porgcoat.2015.08.006.
51. Boubakri A, Guermazi N, Elleuch K, Ayedi HF (2010) Study of UV-aging of thermoplastic polyurethane material. Mater Sci Eng, A 527:1649–1654. https://doi.org/10.1016/j.msea.2010.01.014
52. Soucek MD, Ni H (2002) Nanostructured polyurethane ceramer coatings for aircraft. J Coatings Technol 74:125–134. https://doi.org/10.1007/BF02697952
53. Cai G, Wang H, Jiang D, Dong Z (2018) Degradation of fluorinated polyurethane coating under UVA and salt spray. Part I: Corrosion resistance and morphology. Prog Organic Coat 123:337–349. https://doi.org/10.1016/j.porgcoat.2018.07.025
54. Standard Practice for Evaluating Degree of Rusting on Painted Steel Surfaces, (2024). https://www.astm.org/d0610-08r19.html (Accessed 2 Mar 2024)
55. T.E. e C. Ltda, ABNT NBR 15239 NBR15239 Tratamento de superfícies de aço com, (2024). https://www.target.com.br/produtos/normas-tecnicas/38865/nbr15239-tratamento-de-superficies-de-aco-com-ferramentas-manuais-e-mecanicas (Accessed 2 Mar 2024)
56. Xu Q, Lu Q, Zhu S, Pang R, Shan W (2019) Effect of resins on the salt spray resistance and wet adhesion of two component waterborne polyurethane coating. E Polym 19:444–452. https://doi.org/10.1515/epoly-2019-0046

57. Xie D-M, Lu D-X, Zhao X-L, Li Y-D, Zeng J-B (2021) Sustainable and malleable polyurethane networks from castor oil and vanillin with tunable mechanical properties. Ind Crops Prod 174:114198. https://doi.org/10.1016/j.indcrop.2021.114198